

CMEs and Space Weather

J. G. Luhmann

Space Sciences Laboratory, University of California, Berkeley, California

Although it has been appreciated for some time that solar wind disturbances drive major geomagnetic activity, there is now a better understanding of the solar causes of these disturbances. In particular, the identification of CMEs at the Sun as the primary source of the most "geoeffective" disturbances has given new impetus and inspiration to the space weather forecasting enterprise. Basic research on the CME initiation and propagation processes is expected to lead to improved physical understanding that translates to predictive schemes. The National Space Weather Program Implementation Plan briefly outlines what needs to be done in a set of "bullets" that are repeated here for perspective. These plans aside, we can already see new ideas and data sets in this volume that have the potential to be incorporated into space weather applications, in many ways the ultimate test of our understanding.

1. INTRODUCTION

In the past, solar flares held center stage in descriptions of solar activity effects on the Earth and its technological systems. Without question, the generation of bursts of energetic photons at UV, X-ray and sometimes gamma ray wavelengths produce ionospheric effects within the light travel time of the flares' occurrence on the Sun. Similarly, flare-associated radio bursts interfere with communications around the time of the flare, while probable flare site-accelerated energetic particles produce anomalous ionization in the atmosphere at high latitudes and sometimes add to the satellite radiation environment. Nevertheless, especially since the publication of the consciousness-raising *Journal of Geophysical Research* article by Gosling [Gosling, 1993], new appreciation has been gained for the importance of the less visible coronal eruptions called CMEs in producing "space weather" events. Indeed, as several papers in this volume imply, the

CME phenomenon can be regarded as perhaps the greatest challenge of space weather forecasting. Some of the reasons are briefly reviewed here.

2. GEOMAGNETIC DISTURBANCES: SPACE WEATHER'S STORMS

One has only to look at extended geomagnetic records, like the Dst index interval reproduced in Figure 1 [from Tsurutani *et al.*, 1995], to confirm the episodic nature of space weather. Each major (>100 nT) reduction in this index reflects a decrease in the Earth's surface magnetic field at mid and low latitudes caused by increased currents in the magnetosphere. Experience has taught us that such episodes are generally accompanied by enhanced auroral activity and all of the associated atmospheric, ionospheric, and induced ground-current effects that collectively make a magnetic storm.

It has been understood for some time that solar wind disturbances lead to magnetic storms, and that they have their greatest effects when the disturbance has the combination of large plasma velocities V , and large southward components of the interplanetary magnetic field ($-B_z$). In fact, most physically-inspired solar wind energy

SOLAR WIND – MAGNETIC STORM CORRELATIONS

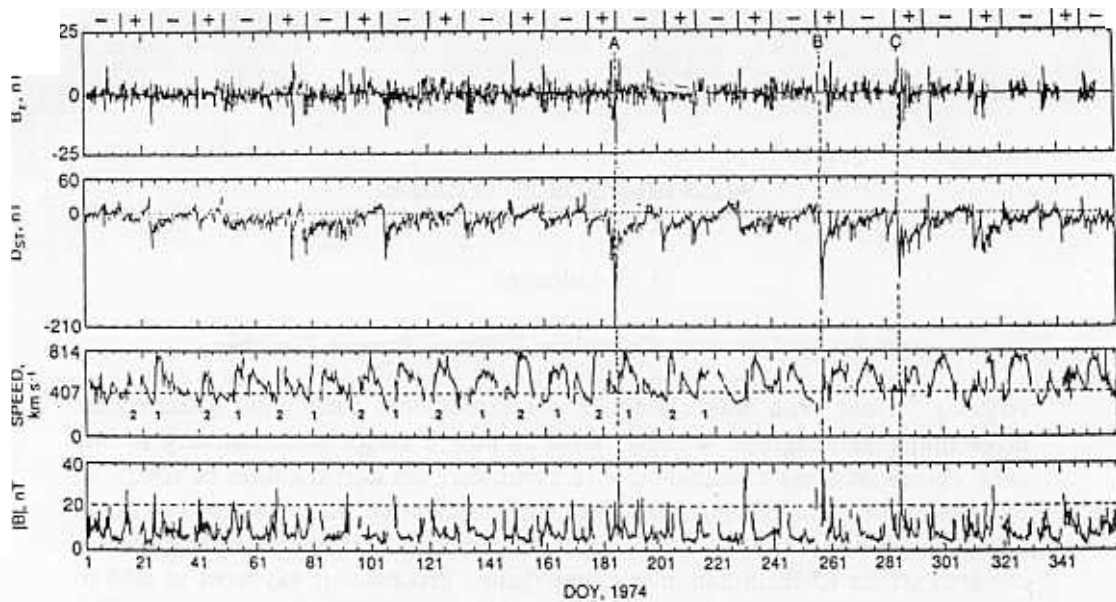


Figure 1. Record of the geomagnetic activity index Dst for the year 1974 [from Tsurutani *et al.*, 1995]. The Dst index is a particularly good measure of major geomagnetic activity, or magnetic storms, because it is heavily based on mid to low latitude ground based magnetic measurements. Key solar wind parameters (velocity and north-south interplanetary field B_z) are also shown. Several large storms are indicated by the dashed vertical lines. Each major Dst disturbance is likely to be the response to arrival of a CME-caused interplanetary disturbance.

or momentum "coupling functions" involve some combination of these two parameters [e.g., Gonzalez *et al.*, 1994]. One particularly popular combination is the product VB_z , which is the component of the solar wind convection electric field ($E = -V \times B$) related to $-B_z$. The physical basis for this choice is illustrated by Figure 2 [from Hughes, 1995]. A southward interplanetary field efficiently interconnects with the Earth's magnetic field, thereby mapping the solar wind electric field into the magnetosphere and ionosphere along the approximately "equipotential" interconnected field lines.

3. INTERPLANETARY DISTURBANCES

The two predominant causes of solar wind disturbances producing intervals of enhanced interplanetary VB_z are CMEs and solar wind stream interaction regions [e.g., Lindsay *et al.*, 1995, and references therein]. The effects associated with a CME in the solar wind near 1 AU and a stream interaction region near 1 AU are illustrated by the examples in Figure 3. Each type of disturbance has a distinctive character corresponding to its physical nature. The CMEs (e.g. Figure 3a), if moving supermagnetosonically with respect to the ambient solar wind, are preceded by an interplanetary shock that is

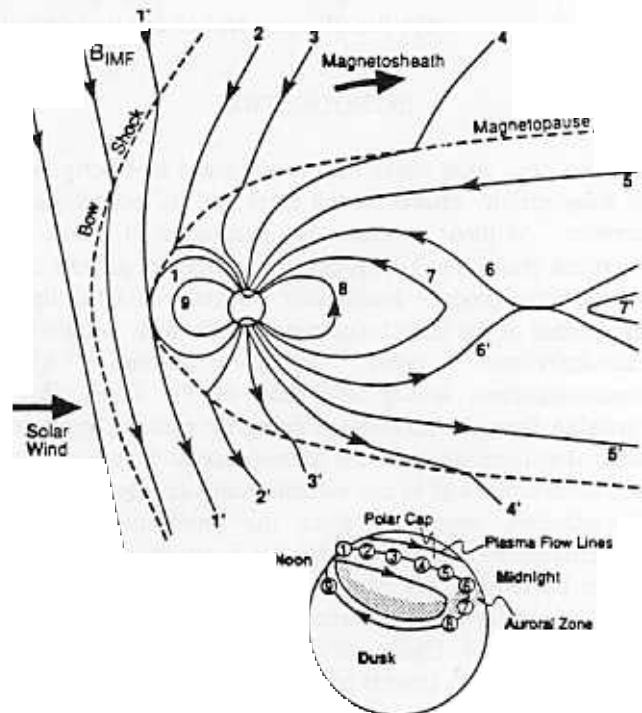


Figure 2. Illustration of how southward interplanetary field interconnects with Earth's field to allow efficient transfer of solar wind energy and momentum to the magnetosphere [from Hughes, 1995].

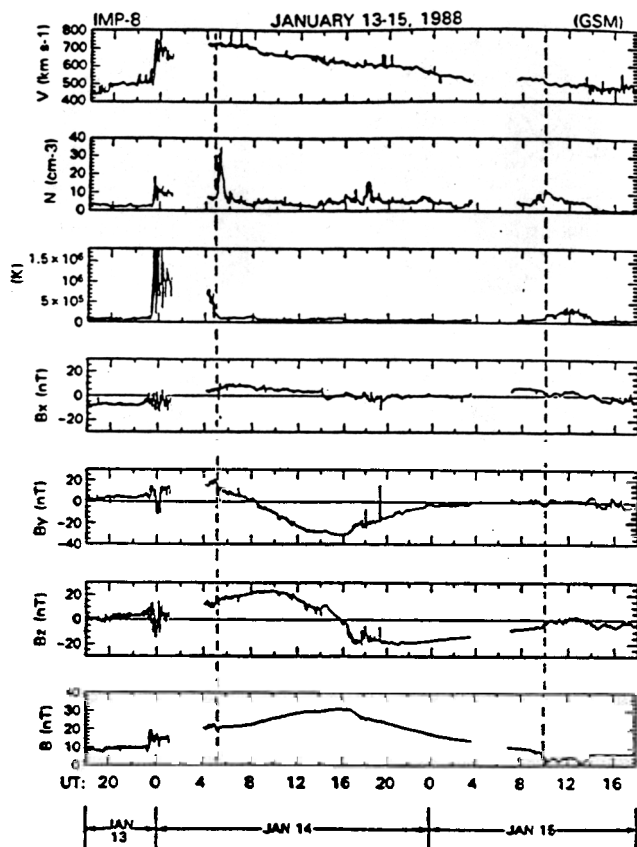
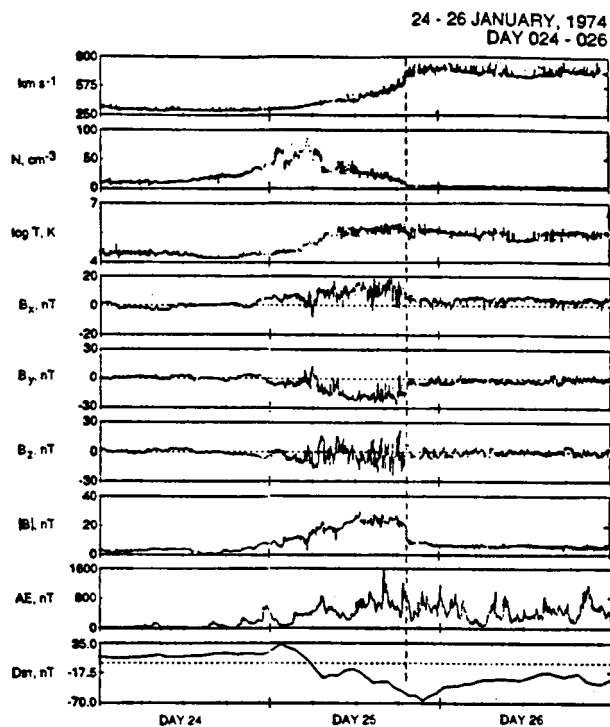


Figure 3a. Example showing the disturbed interplanetary conditions produced by the passage of coronal mass ejecta [from *Farrugia et al.*, 1993].

followed by enhanced density, velocity and magnetic fields reflecting the pile-up of ambient solar wind ahead of the CME as it plows outward. The magnetic field in this "sheath" region is often deflected out of the ecliptic, thereby enhancing its potential "-Bz" contribution [McComas *et al.*, 1989]. The sheath region passage is typically followed by what appears to be the evolved coronal ejecta, another source of enhanced VBz that sometimes resembles a huge flux-rope [see *Marubashi*, this volume]. It should also be appreciated that in addition to the VBz effects caused by fast CMEs, the preceding shocks can act as broad sources of interplanetary energetic particle events.

The stream interaction regions (e.g., Figure 3b), in contrast, are rarely accompanied by shocks at 1 AU. They further tend to have more rapidly fluctuating and smaller Bz enhancements, and the higher velocities, which appear near the end of the interaction region passage, do not necessarily coincide with the largest Bz enhancements.



The $Dst = -65$ nT storm created by a corotating stream/heliospheric current sheet (HCS) interaction

Figure 3b. Example of disturbed interplanetary conditions associated with a particularly strong stream interaction region at 1 AU [from *Tsurutani et al.*, 1995].

This behavior is understood from the different physical nature of the stream interaction, where compression of the slow stream is caused by a highly oblique interaction with the fast stream, and the fast stream is not a discrete entity but rather a part of the general solar wind flow [e.g., *Pizzo*, 1991].

While stream structure disturbances like that in Figure 3b can cause geomagnetic disturbances that affect indices like Dst, and in fact are the likely cause of "recurrent" storms that reappear with the 27 day rotation period of the Sun, they are generally smaller than fast CME disturbances. As seen in the results reproduced in Figure 4, statistical studies of the "geoeffectiveness" parameter VBz in stream interaction regions and CME disturbances show clearly the greater impact of CMEs. Of course *McAllister et al.* [this volume] and others have shown that CME disturbances can be reinforced by interaction with stream structure that magnifies the already enhanced solar wind parameters. These complex or compound disturbances may in fact be responsible for the very largest storms. It is also worthwhile in this context to mention the role of solar

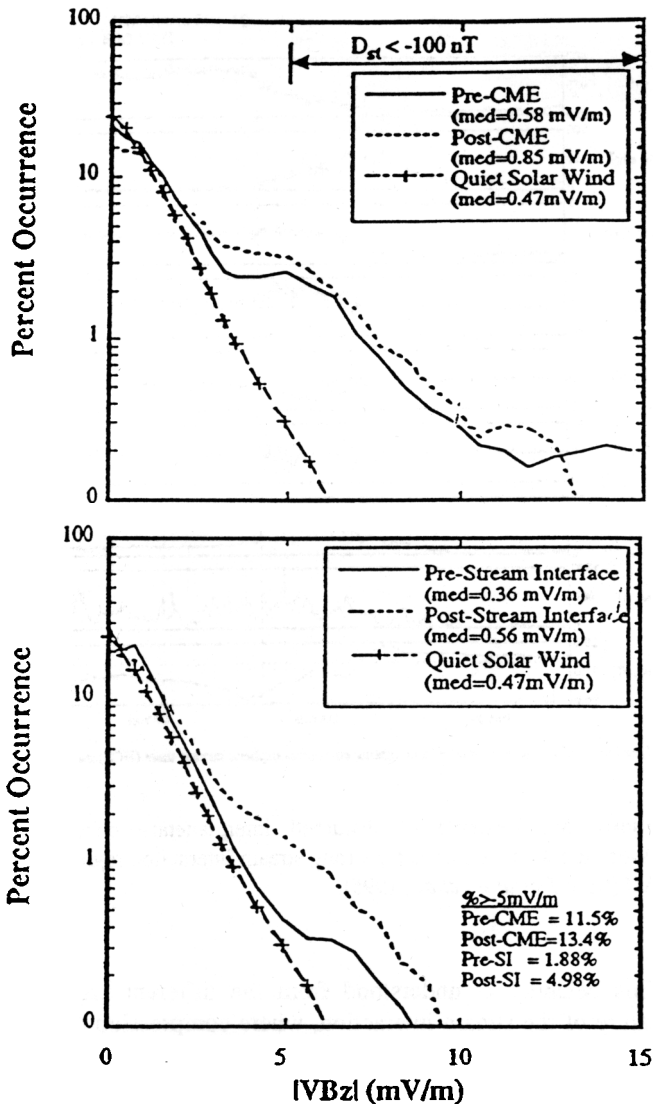


Figure 4. Statistical analysis of the interplanetary parameter VBz associated with passing CMEs and stream interaction regions [from Lindsay *et al.*, 1995]. Note the larger tail on the distribution for CMEs, which make the strongest disturbances.

wind dynamic pressure as it is currently understood. Studies that relate geomagnetic activity indices such as Dst to solar wind parameters find that increases in dynamic pressure can produce disturbances, and can significantly enhance the effects of increased VBz [e.g., Scurry and Russell, 1991]. It has recently been found that in cases where the compression of the magnetosphere occurs suddenly in response to the arrival of an interplanetary shock, transient new radiation belt populations may appear [Blake *et al.*, 1992]. However, large VBz appears to be the primary factor in producing the wide range of space weather effects associated with major storms.

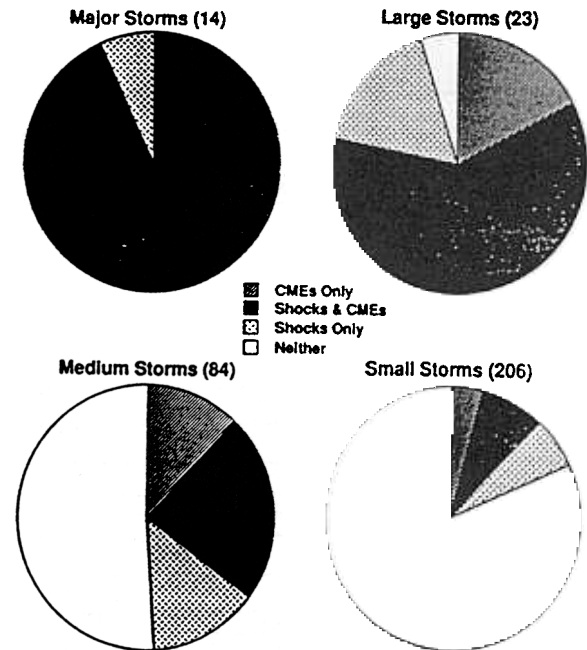


Figure 5. Pie charts from Gosling *et al.* [1991] showing the causes of magnetic storms of various sizes based on analysis of the prevailing interplanetary conditions. (It should be noted that Gosling used a different definition of "major" and "large" storms than is used by the NOAA Space Environmental Center.)

4. THE INTERPLANETARY/GEOMAGNETIC DISTURBANCE CONNECTION

The goal of predicting major geomagnetic activity is of course closely tied to the determination of the cause(s) of large interplanetary VBz. Substantial progress was made when the results contained in the pie charts in Figure 5 [from Gosling *et al.*, 1991] made the CME-magnetic storm connection explicit. Of 14 major and 23 large storms, ~90% and ~65% were associated with some interplanetary signature of a CME disturbance. In many of these cases, a leading interplanetary shock, signalling the passage of a particularly fast cloud of ejecta, provided another measure of geoeffectiveness. Over long time scales, the appearance of a sunspot cycle-phased modulation of many geomagnetic indices, as shown by the example in Figure 6 [from McPherron, 1995], implies the dominance of CMEs as geomagnetic activity drivers. Figure 7 [from Webb and Howard, 1994], and Figure 8 [from Lindsay *et al.*, 1994] in combination show that virtually all signatures of CME occurrence at the Sun and in interplanetary space increase and decrease with the sunspot number. In contrast, the stream interaction-related disturbances occur with a frequency almost in antiphase with the sunspot cycle.

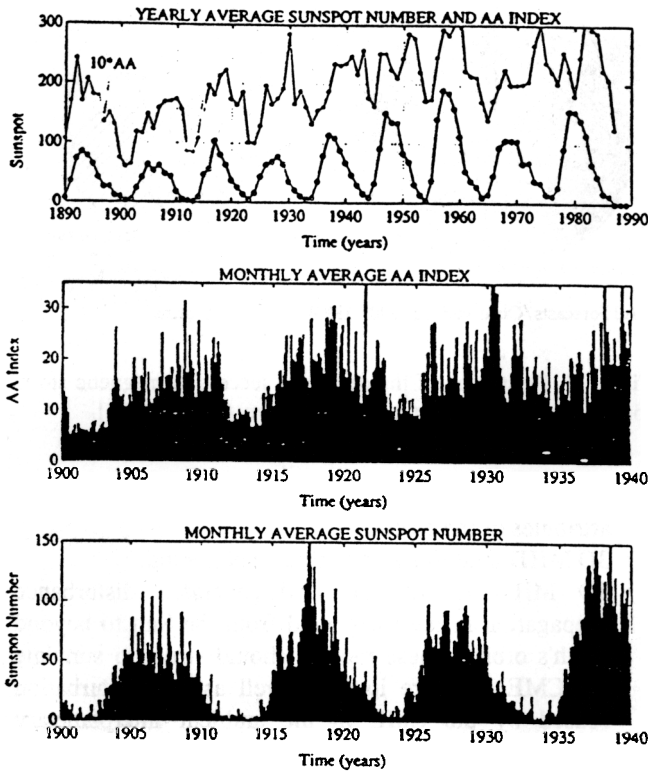


Figure 6. Record showing the solar cycle dependence of the geomagnetic AA index (also based on ground magnetic field deviations) compared to the sunspot number [from McPherron, 1995].

This conclusion regarding CMEs' primary contribution to geomagnetic activity explains the poor record for magnetic storm forecasts mentioned by Hildner and illustrated in Figure 9 [from Joselyn, 1995]. While the preponderance of geomagnetically quiet days can generally be predicted, the chance of accurately predicting the occurrence of a magnetic storm is well-exceeded by the chance of giving a "false alarm" and the chance of missing a storm that occurs. An ability to detect the departure of a potentially geoeffective (e.g., fast), Earth-bound CME at the Sun would probably provide a more noticeable improvement in our forecasting capabilities than any other single accomplishment. This is the essence of why the understanding of CMEs figures so prominently in the plans of the National Space Weather Program.

5. CME GOALS FOR THE SPACE WEATHER PROGRAM

The philosophy behind the National Space Weather Program initiative is to use and improve our physical

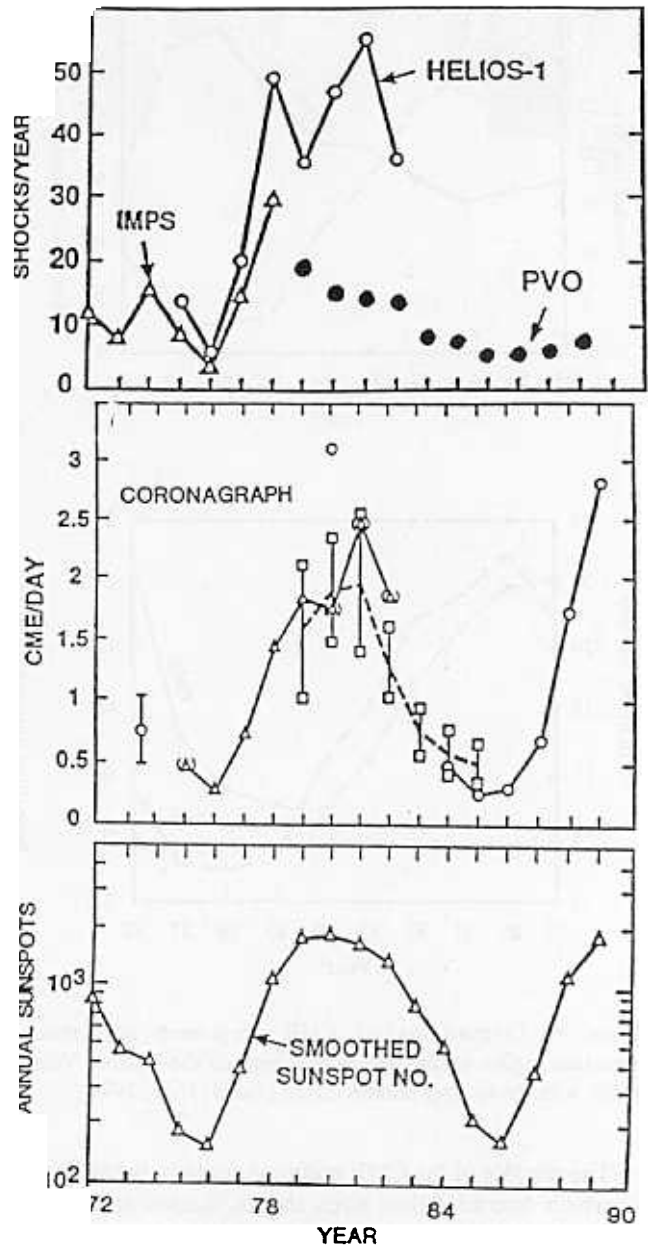


Figure 7. Comparison of CME frequency derived from coronagraph records and interplanetary observations with sunspot number [from Webb and Howard, 1994].

understanding of "space weather" to provide accurate predictions of space environment conditions. The manner in which this challenge can be addressed has been given some attention in the National Space Weather Program Implementation Plan (<http://www.geo.nsf.gov/atm/nswp/nswp.htm>). For CMEs this entails understanding:

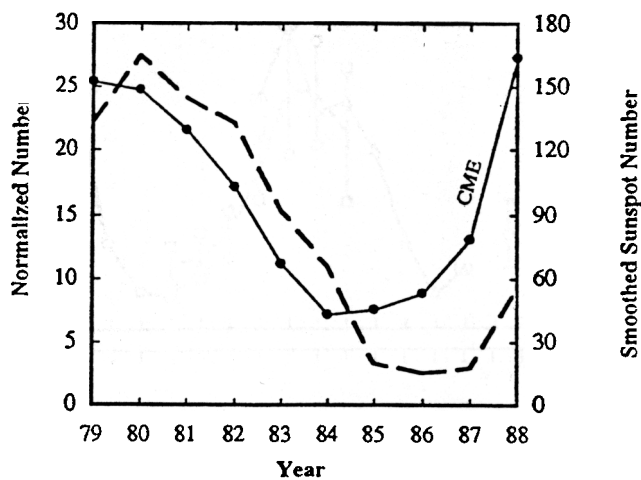
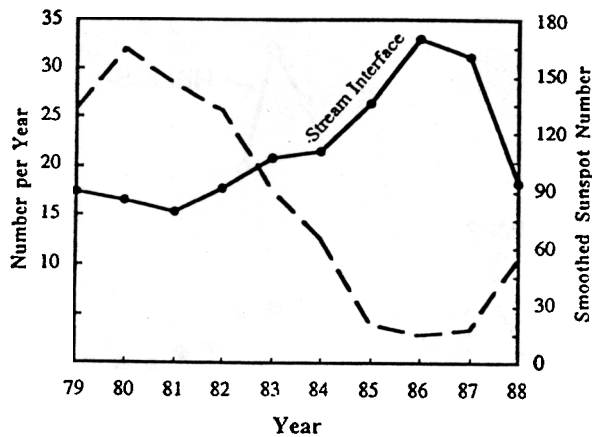


Figure 8. Comparisons of CME occurrence and stream interaction region occurrence as observed on the Pioneer Venus Orbiter with the sunspot number [from Lindsay et al., 1994].

- The physics of the CME initiation process, the factors which determine their sizes, shapes, masses, speeds, and internal field strengths and topologies.
- How to predict the above on the basis of planned observing systems.
- How to predict CME-caused solar wind disturbances and solar energetic particle events near the Earth.

A combination of modeling and observational developments is advocated in the Implementation Plan, the list of which is essentially repeated here:

Models

- Models of the CME initiation process that use realistic observable boundary conditions at the Sun to predict

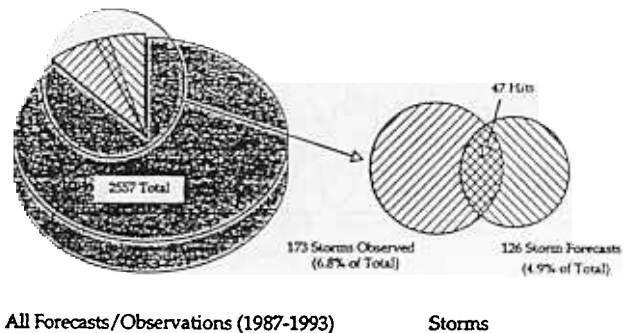


Figure 9. Illustration of the degree of success of magnetic storm forecasting using present techniques [from Joselyn, 1995].

"injection" speed, mass, and intrinsic magnetic field attributes of the ejecta.

- 3D MHD models of the ambient solar wind.
- 3D MHD models of CME-generated disturbance propagation in the solar wind from the Sun to beyond Earth's orbit. These models should strive to simulate the CME structure itself as well as the perturbation caused by the CME in the ambient interplanetary medium. They should ultimately be able to describe disturbance initiation and propagation from the base of the corona to 1 AU using realistic initial conditions for the ambient wind and realistic boundary conditions for the CME disturbance itself.
- 3D models of particle acceleration by CME-driven interplanetary shocks. These models should be capable of predicting the intensity and time history of the CME-associated energetic particle events at 1 AU given a realistic model of the disturbance propagation as in the above bullet.
- Models of the CME-driven shock related radio emission process. These models are needed to optimize the use of radio noise as a remote sensing device and as a diagnostic of approaching CMEs.

Observations

- Soft X-ray imagers for use in understanding and predicting solar wind disturbances such as provided by Yohkoh and SOHO, in anticipation of the SXI X-ray monitoring spacecraft series.
- Radio facilities for tracking solar wind disturbances in interplanetary space from the Sun to the Earth, using both radio bursts and the interplanetary scintillation technique.
- Coronagraphs for studying the behavior of CMEs as a function of radial distance.

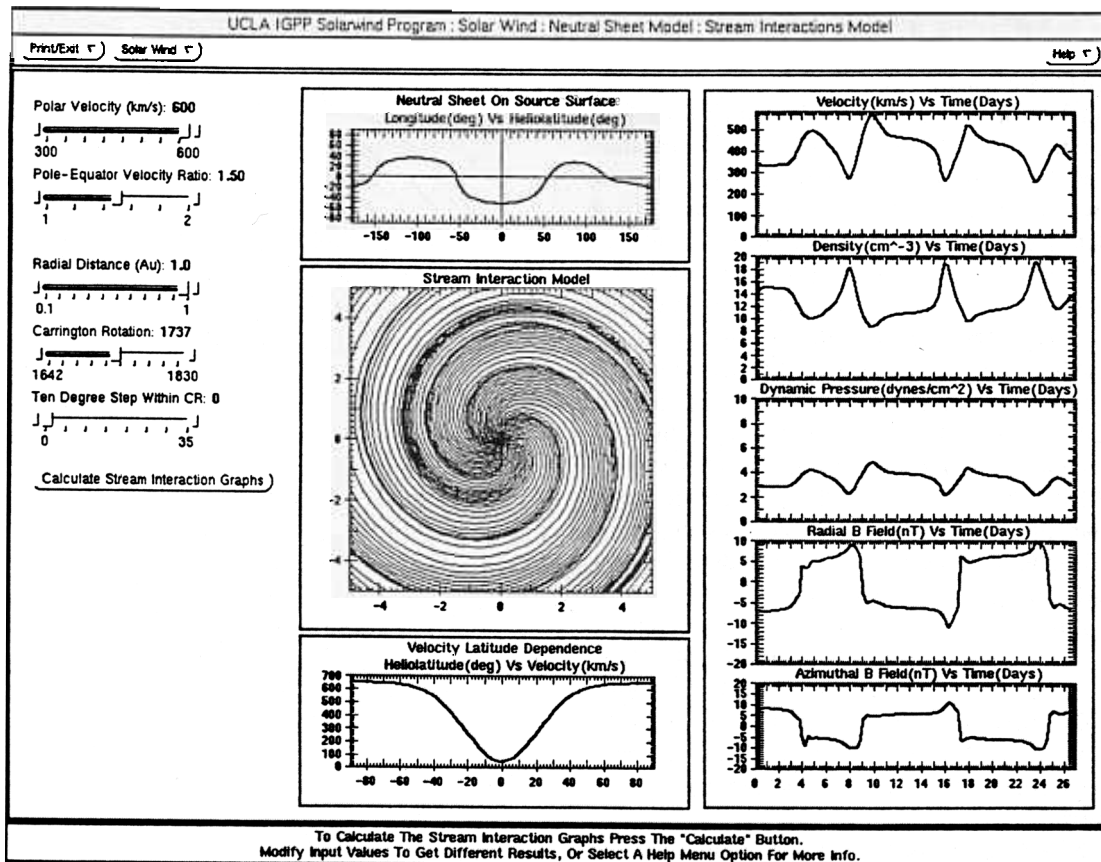


Figure 10. Display from a potential tool for solar wind stream structure forecasting from full-disk magnetogram-derived neutral lines.

- Ground-based coronagraphs to provide a measure of global solar CME activity levels, and to increase the data base for investigations of solar cycle variations of CMEs.
- Solar wind monitors placed near Venus or Mercury orbit for predicting solar wind disturbances near Earth.
- L1 or equivalent upstream monitors for carrying out the above investigations and for providing at least a one-hour forecast for major geomagnetic storms.
- EUV magnetographs for measuring coronal magnetic fields.

Because this list will constantly evolve as new knowledge is incorporated into the National Space Weather Program, it should be viewed only as a current perspective that serves as a "benchmark" at the program's beginning.

6. WHAT WE CAN DO NOW

These challenges and future efforts notwithstanding, there are things that we can do today, with current

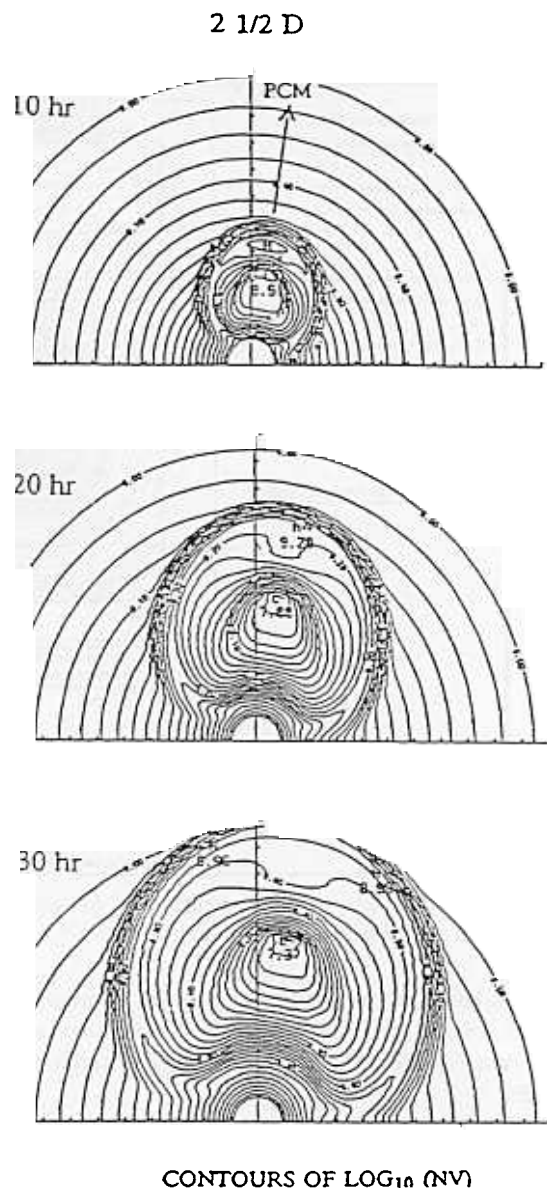
knowledge, to improve the state of the art of CME forecasting. For example, some recent investigations have concentrated on identifying signatures on the Sun that can be used as indicators of a coronal ejection event [e.g., see papers by *Martin and McAllister*, *Hudson and Webb*, *Bothmer and Rust*, among others in this volume]. The association of CMEs with disappearing filaments seen in H-alpha is well-known, while the long duration soft X-ray events, probably arising from the glowing coronal arcades observed in Yohkoh images, seem to follow low coronal disruptions (and sometimes filament disappearances). The newest possibility relates to dimmings of the low corona in the soft X-ray Yohkoh images [see *Hudson and Webb*, this volume]. Of course, one of the problems with the reliance on the filaments is that they are not always present (or seen), while the physical reasons for the soft X-ray arcades and low coronal dimmings are poorly understood. Moreover, the keys to geoeffectiveness, high velocity and substantial southward magnetic field, are not clearly predictable from these "smoking guns" (although *Bothmer and Rust*, [this volume], are optimistic about predicting the

magnetic field orientation when an associated filament is seen). Nevertheless, schemes based on physical models may be available for testing soon.

For example, *Mikic and Linker* [this volume] are able to simulate eruption of realistic coronal helmet streamers subjected to photospheric shearing motions at the footpoints, while *Feynman and Martin* and *Wu et al.* [both this volume] are looking into the role of solar flux emergence in producing CMEs from observational and modeling perspectives. In the meantime, we can make better use of the abundance of new observations of the Sun to gain insight. In particular, the SOHO spacecraft instruments [e.g., see *Howard et al.*, this volume] provide a look at CMEs to several 10s of solar radii from the Sun, with the potential of helping us to understand when and why acceleration of a CME sometimes seems to occur quite far from the Sun. SOHO also provides images in many wavelengths of coronal interest, including full-disk magnetograms every 96 minutes that can be used to analyze the flux emergence concepts. Yohkoh continues to produce more data on the low coronal soft X-ray phenomena it discovered including coronal dimmings. The GONG network, in addition to possible helioseismological insights into the generation process, provides low resolution full disk magnetograms on a 20 minute time-scale.

In short, we have an unprecedented opportunity today to both test our present ideas about CME causes against observations and to use comprehensive solar observations to test new forecasting schemes based on these ideas. One can envision, for example, a system where high time resolution full disk magnetograms are used to observe flux emergence and also to update interplanetary stream structure conditions. The solar wind model might be used to produce a display that looked like Figure 10, for example. Then, if an injection location, width and speed was inferred, even approximately, another model could be used to propagate the transient through the solar wind, as illustrated by Figure 11, at least forecasting the disturbance pressure and velocity and time of arrival. Even the probability of a local shock-accelerated energetic particle event could be given by considering the orientation of the interplanetary field and the strength of the preceding shock [e.g., see *Reames*, this volume]. How we exploit the new observations and our current knowledge is up to us.

Starting next year, the construction phase of the International Space Station (ISS) is scheduled to begin. The ISS has a new high latitude orbit that takes it into the disturbed-time expanded auroral oval to which energetic interplanetary particles have access, and it requires a large number of EVAs to build. At the same time, large



Input Pulses Parameters: $V_s = 2000 \text{ k/s}$, $\omega = 36^\circ$, $\tau = 2 \text{ hr}$

Figure 11. Display from a potential tool for forecasting the properties and timing of CME-driven interplanetary disturbances [from *Smith et al.*, 1992].

networks of navigation and communications satellites such as GPS, Iridium and Teledesic will become essential to our way of life. Solar activity, including the frequency of CMEs, will begin to increase as the 1999-2002 solar maximum is approached. Space weather will become more noticeable. It is a perfect time for us to unravel the physics behind CMEs.

Acknowledgments. The author thanks the conveners for organizing the excellent and timely Bozeman Chapman Conference on CMEs. Her work in this area is supported by NSF grant FD95-31741 from the Solar Terrestrial section of the Atmospheric Sciences Division.

REFERENCES

- Blake, J. B., *et al.*, Injection of electrons and protons with energies of tens of MeV into L<3 on 24 March 1991, *Geophys. Res. Lett.*, 19, 821, 1992.
- Bothmer, V., and D. M. Rust, The field configuration of magnetic clouds and the solar cycle, this volume.
- Farrugia, C.J., M.P. Freeman, L.F. Burlaga, R.P. Lepping, and K. Takahashi, The Earth's magnetosphere under continued forcing: Substorm activity during the passage of an interplanetary magnetic cloud, *J. Geophys. Res.*, 98, 7657, 1993.
- Feynman, J., Evolving magnetic structures and their relation to coronal mass ejections, this volume.
- Gonzalez, W.D., J.A. Joselyn, Y. Kamide, H.W. Kroehl, G. Rostoker, B.T. Tsurutani and V.M. Vasyliunas, What is a geomagnetic storm?, *J. Geophys. Res.*, 99, 5771, 1994.
- Gosling, J.T., The solar flare myth, *J. Geophys. Res.*, 98, 18,937, 1993.
- Gosling, J.T., D.J. McComas, J.L. Phillips, and S.J. Bame, Geomagnetic activity associated with earth passage of interplanetary shock disturbances, *J. Geophys. Res.*, 96, 7831, 1991.
- Howard, R. A. *et al.*, Observations of CMEs from SOHO/LASCO, this volume.
- Hudson, H. S., and D. F. Webb, Ejections of coronal material seen in soft X-rays, this volume.
- Hughes, W.J., The magnetopause, magnetotail, and magnetic reconnection, in *Introduction to Space Physics*, edited by M.G. Kivelson and C.T. Russell, Cambridge Univ. press, New York, 1995.
- Joselyn, J.A., Geomagnetic activity forecasting: The state of the art, *Rev. Geophys.*, 33, 383, 1995.
- Lindsay, G.M., C.T. Russell, J.G. Luhmann, and P. Gazis, On the sources of interplanetary shocks at 0.72 AU, *J. Geophys. Res.*, 99, 11, 1994.
- Lindsay, G.M., C.T. Russell, and J.G. Luhmann, Coronal mass ejection and stream interaction region characteristics and their potential geomagnetic effectiveness, *J. Geophys. Res.*, 100, 16,999, 1995.
- Martin, S., and A. H. McAllister, Predicting the sign of helicity in erupting filaments and coronal mass ejections, this volume.
- Marubashi, K., Interplanetary flux ropes and solar filaments, this volume.
- McAllister, A. H., and N. U. Crooker, Coronal mass ejections, corotating interaction regions, and geomagnetic storms, this volume.
- McComas, D.J., J.T. Gosling, S.J. Bame, E.J. Smith, and H.V. Cane, A test of magnetic field draping induced Bz perturbations ahead of fast coronal mass ejecta, *J. Geophys. Res.*, 94, 1465, 1989.
- McPherron, R.L., Magnetospheric Dynamics, in *Introduction to Space Physics*, edited by M.G. Kivelson and C.T. Russell, Cambridge University Press, New York, 1995.
- Mikic, Z., and J. A. Linker, The initiation of coronal mass ejections by magnetic shear, this volume.
- Pizzo, V., The evolution of corotating stream fronts near the ecliptic plane in the inner solar system 2., Three dimensional tilted dipole fronts, *J. Geophys. Res.*, 96, 5405, 1991.
- Reames, D. V., Energetic particles and the structure of coronal mass ejections, this volume.
- Scurry, L., and C.T. Russell, Proxy studies of energy transfer to the magnetosphere, *J. Geophys. Res.*, 96, 9541, 1991.
- Smith, Z., T. R. Detman, and M. Dryer, Comparison of 2^{1/2}D and 3D simulations of propagating interplanetary shocks, in *Solar Wind Seven*, edited by E. Marsch and R. Schwenn, p. 667, Pergamon Press, Oxford, 1992.
- Tsurutani, B.T., W.D. Gonzalez, A.L.C. Gonzalez, F. Tang, J.K. Arballo, and M. Okada, Interplanetary origin of geomagnetic activity in the declining phase of the solar cycle, *J. Geophys. Res.* 100, 21,717, 1995.
- Webb, D.F., and R.A. Howard, The solar cycle variation of coronal mass ejections and solar wind mass flux, *J. Geophys. Res.*, 99, 4201, 1994.
- Wu, S. T., and W. P. Guo, A self-consistent numerical magnetohydrodynamic model of helmet streamer and flux-rope interactions: Initiation and propagation of coronal mass ejections, this volume.

J. G. Luhmann, Space Sciences Laboratory, University of California, Berkeley, CA 94720-7450.